SOLAR WIND IRON CHARGE STATES OBSERVED WITH HIGH TIME RESOLUTION WITH SOHO/CELIAS/CTOF

M.R. Aellig[1], H. Grünwaldt[2], P. Bochsler[1], P. Wurz[1], S. Hefti[1], R. Kallenbach[1], F.M. Ipavich[3], D. Hovestadt[4], M. Hilchenbach[2], and the CELIAS Team

[1] Physikalisches Institut, University of Bern, Bern, Switzerland
[2] Max-Planck-Institut für Aeronomie, Katlenburg-Lindau, Germany
[3] Dept. of Physics and Astronomy and IPST, University of Maryland, College Park, USA
[4] Max-Planck-Institut für extraterrestrische Physik, Garching, Germany

ABSTRACT

The SOHO/CELIAS/CTOF (Charge Time Of Flight) mass spectrometer measures the ionic and elemental composition of minor ions in the solar wind. From Fe charge spectra we derive the so-called freeze-in temperature with a time resolution of five minutes. Changes in coronal electron temperature as well as in density manifest themselves in a variation of freeze-in temperatures, making the latter a powerful tool for remote coronal diagnostics. Unlike dynamic solar wind properties (velocity, density, kinetic temperature, etc.) the freeze-in temperature of minor ions does not alter on the way from the inner corona to 1 AU.

Variations are observed on timescales down to several hours, sometimes without any substantial change in solar wind plasma parameters. Applying basic plasma diffusion equations, we conclude that the temporal variations in freeze-in temperatures are best explained in terms of spatial variations in coronal conditions. These observations confirm that some of the filamentary structures of the inner corona observed by Koutchmy (1977) survive in the interplanetary medium at least out to 1 AU. Furthermore, we emphasize the prospect to map the *in situ* measured freeze-in temperature back to individual coronal phenomena which are accessible to optical observation.

Key words: solar wind; minor ions; charge states; coronal diagnostics.

1. INTRODUCTION

Matter upstreaming from the photosphere becomes ionized by collisions with hot electrons as it passes the chromosphere and moves into the corona. Both dielectronic and radiative recombination takes place. The rates at which these processes alter the charge state of an ion are all proportional to the electron density n_e since three-body reactions can be neglected. Due to the strong decrease of the electron density with increasing heliocentric distance r the processes changing the ionization state of any ion fade out and the charge state population freezes. Hence, frozen-in charge state spectra of minor ions, e.g. of iron, are powerful tools to detect changes in coronal conditions by remote solar wind *in situ* measurements. This procedure has been outlined earlier, e.g. by Hundhausen (1972) and by Owocki et al. (1983). Here, we summarize the concept of freeze-in temperatures to be used as diagnostic for coronal conditions. In a steadily outflowing solar wind the conservation of particles requires for a given ionization stage i of a species X

$$\nabla \cdot (n_i \mathbf{u_i}) = n_e[n_{i-1}C_{i-1} - n_i(C_i + R_i) + n_{i+1}R_{i+1}] \quad (1)$$

where C_i and R_i denote the temperature-dependent ionization and recombination rate coefficients involving X^{i+}, and n_e and n_i are the densities of electrons and of the species X^{i+}, respectively. The velocity of the ion X^{i+} is denoted by $\mathbf{u_i}$. Eq. 1 defines the characteristic recombination/ionization time of an adjacent pair of ionization stages $i, i+1$ by $\tau_{i \leftrightarrow i+1} = [n_e(C_i + R_{i+1})]^{-1}$. This characteristic time depends on r via the electron density n_e and also via the temperature-dependent rate coefficients C_i, R_{i+1}, and increases with r.

The other characteristic time scale of the solar wind outflow is the expansion time τ_{exp}, i.e. the time it takes ions to flow through one electron density scale height. If we assume the velocity of a given species X to be independent of its degree of ionization i, the expansion time $\tau_{exp} = H/u_i$ is also independent of the charge state i in contrast to $\tau_{i \leftrightarrow i+1}$, which is known to depend on i. Though the electron density scale height varies according to $H \propto r$, the expansion time τ_{exp} decreases with increasing r in the inner corona [e.g. Hundhausen 1972] because the solar wind is strongly accelerated in this region.

The freezing condition is given by

$$\tau_{i \leftrightarrow i+1} = \tau_{exp} \quad (2)$$

where $\tau_{i \leftrightarrow i+1}$ is the characteristic time for modifications of the charge state. Depending on the species

Proceedings of the Fifth SOHO Workshop, 'The Corona and Solar Wind near Minimum Activity', Oslo, Norway, 17-20 June 1997 (ESA SP-404, September 1997)

and the ion pair considered, condition 2 is reached between a fraction of a solar radius and a few solar radii above the solar surface.

The equilibrium condition $X^i \leftrightarrow X^{i+1}$ requires

$$\frac{n_i}{n_{i+1}} = \frac{R_{i+1}(T_e)}{C_i(T_e)} = f_i(T_e) \qquad (3)$$

Applying the simple concept of sudden freezing, we would measure directly the electron temperature T_e at the location where the ion pair $(i, i+1)$ freezes. Since the assumption of equilibrium is not valid in the region where eq. 2 holds, we take the temperature given by eq. 3 as a proxy of the coronal electron temperature at the freezing point. The purpose of this paper is to use the freeze-in temperature as a descriptive parameter. We do not discuss the deviations mentioned above which are caused by the dynamical evolution of the solar wind. Eq. 3 summarizes the scheme of data analysis: The densities of individual iron charge states n_i are derived and the ratio of adjacent ion pairs is used to calculate a freeze-in temperature for the corresponding ion pair. We use the rates given by Arnaud & Raymond (1992), which assume a Maxwellian distribution of the electrons.

The different freeze-in temperatures are fully established a few solar radii above the solar surface, thus they constitute a powerful tool for coronal diagnostic, because they do not change on their way throughout the interplanetary medium, which is in contrast to the dynamical properties of the solar wind such as density, bulk velocity, and thermal velocity.

2. INSTRUMENT DESCRIPTION

The CTOF sensor of the SOHO/CELIAS experiment is a linear time-of-flight mass spectrometer using the carbon foil technique. It is especially designed to separate the individual charge states up to Fe and also to distinguish between different species with the same mass per charge such as Fe^{14+} and Si^{7+}. A more detailed description of the sensor is given by Hovestadt et al. (1995).

The present data analysis relies on an instrument response model and on a maximum likelihood inversion algorithm used by Aellig (1997) that yields densities of the individual charge states of iron with an error estimate. For this purpose we use so-called matrix elements that sum the counts accumulated during a full instrument cycle in rectangular regions of the mass and mass per charge domain.

3. RESULTS

As outlined in the previous sections, densities of the individual charge states have been calculated from the matrix elements. By taking the density ratios of adjacent charge states, freeze-in temperatures $T_{i+1,i}$ for these pairs have been derived according to eq. 3. The three freeze-in temperatures $T_{10,9}$, $T_{11,10}$, and $T_{12,11}$ determined in the time period between

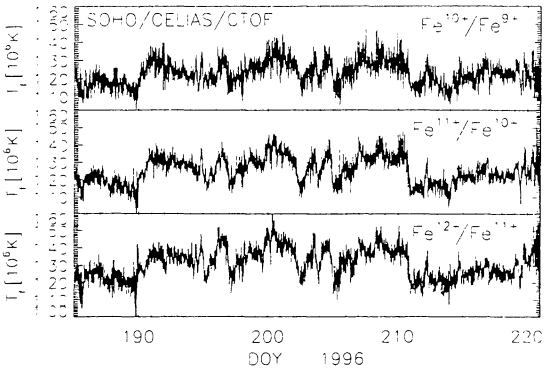

Figure 1. Freeze-in temperatures derived from the ratios of different iron charge state densities. Note the short-scaled peaks and the steep gradients of the consistently varying freeze-in temperatures.

DOY 185 and DOY 220 in 1996 are shown in Figure 1. The data shown have been calculated with the maximum time resolution of five minutes and were then smoothed with a boxcar average of 25 minutes' width. First we note that the three freeze-in temperatures show common rapid and correlated variations down to very short time scales. This applies, for example, to the steep gradient observed on DOY 210 and to the short-scale change on DOY 212, which is the subject of a closer investigation. Due to the high time resolution it is possible to investigate not only large-scale structures such as coronal holes but also to study smaller structures.

Less obvious from Figure 1 is the fact that the freeze-in temperatures differ for each ion pair. The mean freeze-in temperature for the pair Fe^{10+}/Fe^{9+} in the period shown in Figure 1 amounts to $\overline{T}_{10,9} = 1.22 \times 10^6$ K, for the pair Fe^{11+}/Fe^{10+} to $\overline{T}_{11,10} = 1.25 \times 10^6$ K, and to $\overline{T}_{12,11} = 1.31 \times 10^6$ K for Fe^{12+}/Fe^{11+}, respectively. This is consistent with the picture that, generally, the higher charged pairs freeze closer to the Sun due to their shorter characteristic time $\tau_{i \leftrightarrow i+1}$.

In Figure 2 a closer view of the short-scaled peak on DOY 212 in all three freeze-in temperatures is presented. To assess the characteristic duration of this event, a Gaussian with a characteristic one sigma width τ_i superposed on a baseline was fitted to the data. We estimate the characteristic duration τ of the event to be 2 h.

The amplitude of the superposed signal is about 1×10^5 K in all three cases, which corresponds to a change of less than 10% in the freeze-in temperature domain. However, if we translate this increase in a change of the density ratio the effect is stronger. To account for the increase from about 1.20×10^6 K to 1.32×10^6 K the density ratio Fe^{12+}/Fe^{11+} has to change by almost 50%.

4. DISCUSSION

One of the first questions to discuss concerning the peak in freeze-in temperatures is if it was caused by a

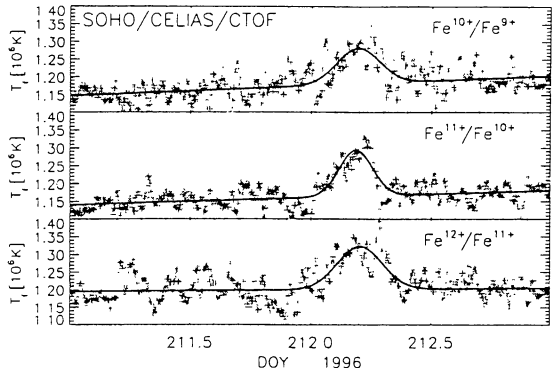

Figure 2. The same freeze-in temperatures as shown in Figure 1 zoomed around DOY 212 in 1996. A highly significant peak is centred around DOY 212.2. The freeze-in temperatures $T_{f,i}$ were fitted in all three cases with a Gaussian of variable one sigma width τ_i superposed on a baseline.

transient event or by a lateral change of coronal conditions. The two scenarios are schematically shown in Figure 3. In the case of a transient event, solar wind "marked" by a high freeze-in temperature passes by SOHO like a large cloud, whereas in the case of a lateral variation on the solar surface, the especially "labelled" solar wind has the shape of the ray from a turning lighthouse which hits SOHO. The peak in the freeze-in temperatures will be referred to as signal which is injected into the solar wind plasma. In the

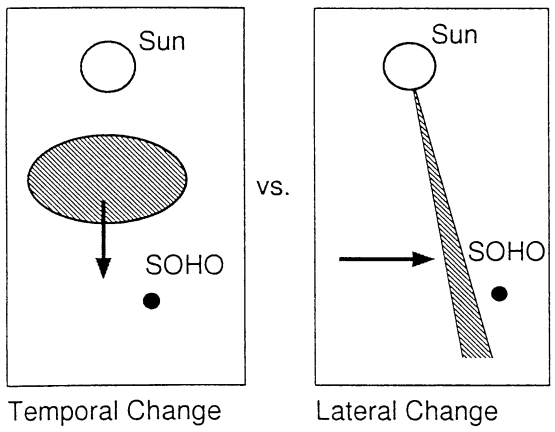

Figure 3. Both temporal and lateral changes in coronal conditions may lead to a transient peak of freeze-in temperatures as shown in Figure 2. Additional analysis of parameters such as the thermal velocity is required to assess which scenario applies.

following subsections the two scenarios are analyzed in more detail.

4.1. Temporal Variation of Coronal Conditions

If we assume the solar wind to be collisionless on its way from several $R_\odot$ to 1 AU, we can estimate the expected signal width from the thermal velocity v_{th} and the solar wind bulk speed v_{sw} for the case of temporal variations of coronal parameters. A sharp signal injected into the solar wind a few solar radii above the solar surface will have a temporal width s_t at a radial distance r

$$s_t \approx \frac{v_{th} r}{v_{sw}^2} = \frac{v_{th}}{v_{sw}} t_{tr} \qquad (4)$$

where $t_{tr} = r/v_{sw}$ equals the transit time of the solar wind from the Sun to the radial position r assuming constant velocity. Contrary to diffusion, where collisions occur, $s_t \propto t$ rather than $s_t \propto t^{1/2}$ as expected for diffusion. For the specific feature on day 212 in 1996 we have for the protons $v_{th} = 20$ km s^{-1} derived from SOHO/CELIAS/PM data and for the heavy ions the values commensurate with the proton thermal velocity except for a short dip of half an hour which is less prominent for iron than for oxygen [Hefti 1997]. The rough estimate in eq. 4 is conservative since the thermal velocities are known to generally decrease with heliocentric distance r. On the other hand the bulk velocity increases with increasing r. The correct way to evaluate s_t is to integrate $v_{th} v_{sw}^{-2}$ along the travel path of the solar wind. The integration would start at the time where the charge states freeze and thus "mark" the solar wind. Evidently, the integrand is quite large in the corona just after the freezing-in point, since the ion temperature is much higher than at Earth's orbit and the solar wind is still quite slow, i.e. of the order of 100 km s^{-1}. Therefore, it is safe to calculate s_t with the parameter values determined at 1 AU by SOHO/CELIAS/PM. The solar wind bulk velocity was found to be approximately 380 km s^{-1} at this time which yields a time width s_t at Earth's orbit of $s_t \approx 6$ h. This value exceeds the observed width of $\tau \approx 2$ h significantly. From the rough estimate we rule out the case of a wave-like dispersed signal as shown schematically on the left side of Figure 3.

4.2. Lateral Variation of Coronal Conditions

In this section the possibility of lateral variation of coronal conditions is discussed. The width of the signal may be interpreted in two extreme and opposite views.

- Assuming that no perpendicular diffusion occurred on the way from the solar corona to 1 AU, the original structure size in the corona can be estimated.
- The signal observed at 1 AU is due to a small structure broadened by perpendicular diffusion. This allows to estimate an upper limit for the perpendicular diffusion coefficient.

In the first case the size L of the signal emitting structure located a radial distance $r/R_\odot$ is calculated from

simple geometric arguments to be

$$L = \frac{r}{R_\odot} \frac{2\pi R_\odot}{T_{rot}} \tau \qquad (5)$$

Mapped back onto the solar surface the typical one sigma length is approximately 15'000 km, which is of the same order as the supergranulation. Since freezing occurs a few solar radii above the surface the typical length scale has to be multiplied by the height at which the charge spectra freeze.

The second point of view is adopted for the following discussion. We start by discussing three different mechanisms that give rise to perpendicular diffusion and thus lead to a broadening of a lightbeam-like signal. The processes considered are:

- Diffusion perpendicular to $\vec{B}$ due to particle collisions
- Resonant scattering at small-scale irregularities of the $\vec{B}$-field
- Field line mixing

Whereas encounters between ions and electrons reduce diffusion along the magnetic field, they are needed for particles to diffuse perpendicular to the magnetic field, otherwise any ion would remain on the field line on which it started. Since collisions are extremely rare in the solar wind, one could think that this process is unimportant. This was checked by transforming the diffusion length scale L_d as estimated from Burgers (1969) into a timescale τ_d of the signal observed in the solar wind using $L_d = \tau_d \omega_\odot r$, where $\omega_\odot$ denotes the rotational speed of the Sun. Although the case considered was diffusion of plasma into free space permeated by a magnetic field, we found $\tau_d \ll \tau$. Again our estimate is conservative since in the case of iron ions, we do not necessarily have a pressure gradient to drive diffusion as assumed for the calculation of τ_d. If diffusion perpendicular to the magnetic field is due to particle collisions only, the observed freeze-in temperature pattern is a close image of the coronal conditions that is not blurred during its transport throughout interplanetary space. This sight is unrealistic since for these estimates completely undisturbed velocity and magnetic fields are assumed.

Resonant scattering of particles at magnetic irregularities is an important process for the propagation of cosmic rays, e.g. Jokipii (1966), and could also apply to the perpendicular diffusion of the freeze-in temperature signal. Significant scattering of particles occurs only if their gyroradius has the same scale as the irregularity of the magnetic field. Since solar wind ions have much smaller gyroradii than cosmic ray particles, they are scattered by smaller spatial irregularities. Shorter wavelength means, e.g. for Alfvén waves, higher frequency, where the power spectral density of the magnetic field fluctuations is much smaller. As noted by Jokipii & Parker 1969 resonant scattering is negligible compared to field line mixing for the perpendicular diffusion of low rigidity particles. We extrapolate this statement to solar wind ions, where the cyclotron motion is caused by the thermal velocity of the particles.

We now discuss the influence of field line mixing upon the perpendicular diffusion. Applied to the problem of the broadening of the freeze-in temperature signal, this means that individual field lines are marked with a high freeze-in temperature T_f. A high T_f results from a high density ratio of adjacent charge states. By the mixing of field lines this density ratio changes, and therefore also T_f. We use the width τ of the T_f signal to estimate the diffusion coefficient of particles perpendicular to the magnetic field $\kappa_\perp$ due to field line mixing. The perpendicular transport is caused by the mixing of the field lines only, since the particles are assumed to be tied to the individual field lines. From the fact that field line mixing is caused by the random walk of the footpoints of the magnetic field in the photosphere, Jokipii and Parker concluded that the random walk coefficient

$$c_{rw} = \frac{\langle (\Delta x)^2 \rangle}{\Delta z} \propto r^2 \qquad \text{for } r \leq 1 \text{ AU} \qquad (6)$$

The random walk coefficient indicates the mean quadratic displacement perpendicular to the magnetic field per distance Δz moved along the field. Using eq. 5 to estimate the spatial extent of the signal at Earth's orbit, the proportionality in expression 6 and by integration of the random walk coefficient from the Sun to Earth's orbit we estimate its value at Earth's orbit to be

$$\left. \frac{\langle (\Delta x)^2 \rangle}{\Delta z} \right|_{R=1AU} \leq 9 \times 10^7 \text{m} \qquad (7)$$

which is a factor of six below the value estimated by Jokipii and Parker. Note that this is an upper limit, since the size of the source region of the freeze-in signal is assumed to vanish.

In view of this difference the following comments are made. Jokipii and Parker use the spectral power at zero frequency to estimate the random walk coefficient based on magnetic field data from 1964. This value may well be different during the time period in which our signal was recorded. Additionally, and more importantly, the size of the structure observed in the freeze-in temperature is of the same order of magnitude as the correlation length of the magnetic field fluctuations determined by Jokipii and Parker. This could also explain our lower random walk coefficient.

We derive the perpendicular diffusion coefficient $\kappa_\perp$ for solar wind ions in a similar way as we did for c_{rw}. In addition to the same radial dependence for $\kappa_\perp$ as for c_{rw}, a constant solar wind bulk speed of $v_{sw} = 380$ km s^{-1} is assumed. Then the upper limit for the diffusion coefficient $\kappa_\perp$ is calculated to be

$$\kappa_\perp|_{R=1AU} \leq 6 \times 10^{13} \text{ m}^2 \text{ s}^{-1} \qquad (8)$$

5. SUMMARY AND CONCLUSIONS

We have shown that the iron freeze-in temperatures from the SOHO/CELIAS/CTOF mass spectrometer show rapid variations and steep gradients indicating

small-scaled changes in coronal conditions. One single event, a short increase of three Fe freeze-in temperatures, was analyzed in more detail. The observed signature is explained with a lateral change in coronal conditions rather than with a temporal variation. With the assumption that the high freeze-in temperature signal originates from a small source region, three different mechanisms of diffusion perpendicular to the magnetic field were discussed and their relative importance was assessed. For the magnetic field line mixing dominated scenario, an upper limit for the field line random-walk rate $c_{rw} = 9 \times 10^7$ m is found, which is a factor of 6 below the value by Jokipii & Parker (1969). Two possible reasons for this disagreement were discussed. The derived diffusion coefficient for perpendicular motion of solar wind ions shows that, although broadening of a signal injected into the solar wind occurs, we get at Earth's orbit an image which is only slightly blurred. With an instrument sensitive enough such as the SOHO/CELIAS/CTOF mass spectrometer, this allows to detect in the solar wind not only large scale changes in the corona but also small scale changes and to map them back onto the solar surface.

ACKNOWLEDGMENTS

This work was supported by the Swiss National Science Foundation and by DARA, Germany.

REFERENCES

Aellig, M.R., 1997, PhD Thesis, University of Bern, Switzerland

Arnaud, M., Raymond, J., 1992, ApJ, 398, 394

Burgers, J.M., 1969, Flow equations for composite gases, Academic Press

Hefti, S., 1997, PhD Thesis, University of Bern, Switzerland

Hovestadt, D. et al., 1995, Solar Physics, 162, 441-481.

Hundhausen, A.J., 1972, Coronal expansion and solar wind, Springer Verlag.

Jokipii, J.R., 1966, ApJ, 146, 480

Jokipii, J.R., Parker, E.N., 1969, ApJ, 155, 777

Koutchmy, S., 1977, Sol. Phys., 51, 399

Owocki, S.P., Holzer, T.E., and Hundhausen, A.J., 1983 ApJ, 275, 354